

Potential Scattering and Spectroscopic Factors in R -Matrix Theory*

G. D. Westin and J. L. Adams

Department of Physics, Ohio University, Athens, Ohio 45701

(Received 29 April 1971)

The R -matrix theory of nuclear scattering is used to consider the meaning of spectroscopic factors for unbound states. Potential scattering is explicitly calculated by constructing an R function which is equivalent to the potential. The compound effects are then parametrized in the usual R -matrix fashion with the spectroscopic factors being explicitly included as parameters. The spectroscopic factors are found by fitting data. The spectroscopic factors are very sensitive to the choice of the various resonance parameters, and the validity of spectroscopic factors as a meaningful quantity for unbound states is discussed in the light of several calculations. Several types of resonances found in the reactions $^{12}\text{C}(n, n)^{12}\text{C}$ and $^{16}\text{O}(n, n)^{16}\text{O}$ are considered. These include the cases of very narrow and very broad resonances and a double-resonance situation.

I. INTRODUCTION

The study of (d, p) and other particle-transfer reactions in the continuum has been of much interest to both experimentalists and theorists.¹⁻¹² In a normal bound-state (d, p) stripping calculation, the spectroscopic factor of the observed states is found as a normalization factor when theory is compared with experiment. The radial integral encountered in bound-state (d, p) stripping theories is finite because the neutron wave function goes to zero as the neutron radial coordinate goes to infinity. In (d, p) stripping to the continuum the neutron wave function is that for a free state, and the bound-state theory must be modified. Exactly how this can best be done has been the subject of several papers.⁴⁻¹²

The states seen in (d, p) stripping to the continuum can also be seen in neutron elastic scattering as resonances. If spectroscopic factors are computed for these neutron elastic scattering resonances, they should compare with those found in (d, p) stripping to the continuum. All this, of course, assumes that in the continuum the spectroscopic factor is a meaningful physical quantity.

One of the best-known theories of resonance reactions is the R -matrix theory. This theory uses as its parameters the wave function squared and its logarithmic derivative at a radius outside the region of nuclear interaction. In its usual simplified form, the R -matrix theory contains no interaction. The reason for this is that the interaction is so complicated that it cannot be found. The corresponding resonances are frequently very narrow and bear little resemblance to scattering by a potential well. When only the neutron elastic scattering channel is allowed, the R matrix reduces to an R function, and if an isolated resonance labeled λ is considered, the R function is taken to be

$$R = R_0 + \gamma_\lambda^2 / (E_\lambda - E). \quad (1)$$

In this formula, γ_λ^2 is called the reduced width, and E_λ is connected with the energy at which the resonance is seen experimentally. The parameter R_0 is assumed to be independent of the energy. It describes the background effects, and it is frequently taken to be zero. The conventional R -matrix theory works well for narrow, isolated resonances which represent very complicated compound states. However, when the resonances can be described by a potential, and spectroscopic factors are desired, the R -matrix theory needs to be carefully applied.

In this paper we show how potential scattering can be described by the R -matrix formalism. At any given energy, the R -matrix formalism is equivalent to an exact calculation of the scattering from a potential. The single-channel R -matrix parameters at the given energy are the background R_0 , the potential resonance reduced width $\tilde{\gamma}_p^2$ and energy E_p , the R -matrix radius a_c , and the boundary condition b_c . For a range of energies of several MeV, the R function for the one-channel case of potential scattering can be written in the form

$$R^{\text{pot}} = \sum \tilde{\gamma}_p^2 / (E_p - E) \quad (2)$$

$$= R_0 + \tilde{\gamma}_1^2 / (E_1 - E), \quad (3)$$

where the label 1 refers to the single-particle resonance in the region of interest, and the background R_0 can be easily calculated.

Once the potential resonance scattering is parametrized in terms of R -matrix parameters, the experimental data can be fitted using different values for the reduced widths and energies of the resonances. By comparing the potential scattering parameters to the experimental fitting parameters, the spectroscopic factor for a resonance can be defined. However, it turns out that in some cases

the spectroscopic factor so defined is very sensitive to the various parameters chosen. Thus, it may not make very much sense to consider spectroscopic factors when referring to certain resonances.

In Sec. II we show how the conventional R -matrix theory must be applied in order to include potential scattering explicitly. In this section we also derive the simple formulas used by experimentalists in fitting data and discuss how a spectroscopic factor can be found. In Sec. III we apply the formalism to the $d_{3/2}$ double resonance seen in the $^{12}\text{C}(n, n)^{12}\text{C}$ reaction. In Sec. IV we do the same for the very narrow $d_{5/2}$ resonance seen in $^{12}\text{C}(n, n)^{12}\text{C}$. Section V examines the narrow $d_{3/2}$ resonance in $^{16}\text{O}(n, n)^{16}\text{O}$ which can be described by potential scattering. In Sec. VI we examine an $s_{1/2}$ resonance dip in $^{16}\text{O}(n, n)^{16}\text{O}$. A discussion of our results is given in Sec. VII.

II. THEORY

In this section we want to derive the simple formulas normally used by experimentalists in analyzing neutron elastic scattering. We confine ourselves to reactions in which only the elastic scattering channel is open. Two such examples are $^{12}\text{C}(n, n)^{12}\text{C}$ and $^{16}\text{O}(n, n)^{16}\text{O}$.

The $^{12}\text{C}(n, n)^{12}\text{C}$ and $^{16}\text{O}(n, n)^{16}\text{O}$ data are especially interesting because the basic shapes of the excitation functions (cross section vs energy) can be fitted using a real Woods-Saxon potential including spin-orbit effects. When this is done, not only is the background fitted, but also a $d_{3/2}$ resonance at low energy is fitted by the potential. Thus, we say that these $d_{3/2}$ resonances in $^{12}\text{C}(n, n)^{12}\text{C}$ and $^{16}\text{O}(n, n)^{16}\text{O}$ are potential resonances. These are also frequently called single-particle resonances. The background cross sections in these two reactions are due mostly to an s -wave state which is slightly bound.

If we treat the reactions as a simple problem of a neutron being scattered by a potential, we can easily find the solution. The Schrödinger radial equation is

$$(T + V_{\text{W.S.}})u(r_c) = Eu(r_c), \quad (4)$$

where T is the kinetic-energy operator, E is the energy of the neutron in the center-of-mass system, $u(r_c)$ is the wave function of the neutron in the potential, the coordinate r_c is the distance of the neutron from the center of the potential, and $V_{\text{W.S.}}$ is a real Woods-Saxon potential with a surface spin-orbit term. The potential has a central depth V_0 , a spin-orbit depth V_{s_0} , a diffuseness a , and a radius R .

Equation (4) can be solved easily with the aid of

a computer. We use the phase convention that if $V_{\text{W.S.}}$ is real, $u(r_c)$ is real. By varying the parameters, the data can be reproduced reasonably well. Figures 1 and 2 show fits to the $^{12}\text{C}(n, n)^{12}\text{C}$ and $^{16}\text{O}(n, n)^{16}\text{O}$ data from about 0.5 to 4 MeV. From these figures we can see that the over-all shapes of the excitation functions can be fitted with a very simple local potential with no energy dependence. This is very satisfactory, since we know that, in general, the potential is nonlocal or local and energy dependent. Our task is to improve this fit by including compound resonances, using the framework of R -matrix theory. But first, we must consider how the potential calculation can be reproduced using parameters from R -matrix theory.

A. Potential Scattering Using the R Function

The R -matrix theory of nuclear reactions¹³ can easily be used to fit potential scattering. Each partial wave is afforded a separate treatment in R -matrix theory. When the partial waves are summed in the appropriate manner, a cross section results. When fitting neutron-resonance data, we will want to modify only the partial waves which cause resonances in the energy region we are fitting. For instance, if we are trying to fit the low-energy $^{12}\text{C}(n, n)^{12}\text{C}$ data, only the $d_{5/2}$ and $d_{3/2}$ partial waves need to be modified, since they are the partial waves which give rise to resonances. For all the other partial waves, we will use the scattering matrix elements generated by the potential.

Now let us consider the $^{12}\text{C}(n, n)^{12}\text{C}$ data in the region of 3.5 MeV. We see a single-particle resonance caused by the $d_{3/2}$ partial wave. We want to parametrize this in terms of an R function. Before doing this, let us recall some of the R -matrix theory for a single channel.

We can write the radial Schrödinger equation in the interior region $r_c \leq a_c$ as

$$(T + V_{\text{W.S.}})u_p(r_c) = E_p u_p(r_c), \quad (5)$$

where the radial wave function $u_p(r_c)$ obeys the boundary condition

$$\frac{a_c}{u_p(a_c)} [u_p'(r_c)]_{a_c} = b_c, \quad (6)$$

where a prime denotes differentiation with respect to r_c .

In Eq. (4) an energy-dependent quantity similar to b_c can be defined. We call this quantity f_c , where

$$f_c(E) = \frac{a_c}{u(a_c)} [u'(r_c)]_{a_c}. \quad (7)$$

We see then that whenever $E = E_p$,

$$b_c = f_c(E_p) \quad (8)$$

and

$$u_p(r_c) = u(r_c), \quad E = E_p. \quad (9)$$

In the single-channel R -matrix theory, the R function for potential scattering from $V_{w.s.}$ in the $d_{3/2}$ channel is found to be

$$R^{\text{pot}} = \sum_p \frac{\tilde{\gamma}_p^2}{E_p - E}, \quad (10)$$

where the E_p satisfy Eqs. (5) and (6) and

$$\tilde{\gamma}_p^2 = \frac{\hbar^2}{2m a_c} u_p^2(a_c). \quad (11)$$

In general, we are only interested in a particular single-particle state; for instance, the $d_{3/2}$ single-particle state at 3.5 MeV. Near the energy of interest, one term in the series of Eq. (10) will be dominant. The rest can be assumed to be weakly energy dependent. We then write

$$R^{\text{pot}} = R_0(E) + \frac{\tilde{\gamma}_1^2}{E_1 - E}, \quad (12)$$

where E_1 is chosen to be in the region of interest and

$$R_0(E) = \sum_{p \neq 1} \frac{\tilde{\gamma}_p^2}{E_p - E}. \quad (13)$$

Our boundary condition is also determined by our choice of E_1 . It is from Eq. (8):

$$b_c = f_c(E_1). \quad (14)$$

Note that since $u(r_c)$ is chosen to be real, b_c will also be real.

Now, we need to compute the quantity $R_0(E)$ in Eq. (12) to find R^{pot} . This can be done using a method due to Buttle.¹⁴ We recall that R^{pot} can be written

$$R^{\text{pot}} = \frac{1}{f_c(E) - b_c}. \quad (15)$$

Here f_c is an energy-dependent quantity, while b_c is determined once the potential $V_{w.s.}$ and the energy E_1 and the R -matrix radius a_c are chosen. Using Eqs. (12) and (15) we now can find $R_0(E)$:

$$R_0(E) = \frac{1}{f_c(E) - b_c} - \frac{\tilde{\gamma}_1^2}{E_1 - E}. \quad (16)$$

Equation (16) is of use only if $R_0(E)$ is weakly energy dependent. We find $R_0(E)$ by solving Eq. (16) at several energies near E_1 . If R_0 is weakly energy dependent, we can approximate Eq. (12) by

$$R^{\text{pot}} \approx R_0 + \frac{\tilde{\gamma}_1^2}{E_1 - E}. \quad (17)$$

Let us briefly review what we have done. If we consider only the region $r_c \leq a_c$, where a_c is outside the range of the potential $V_{w.s.}$, we can parametrize the scattering from the potential in terms of an energy-dependent R function. This energy-dependent R function is given by Eq. (10) or (15). However, the beauty of the R function is that it can be approximated by a form in which the energy dependence is explicitly seen. This is Eq. (17). In Eq. (17), R_0 and $\tilde{\gamma}_1^2$ are assumed energy independent. The energy dependence is explicitly given by the denominator of the last term.

It is good to remember that in finding the cross section for a single partial wave, Eq. (17) does not stand alone. The quantity b_c also enters into the calculation of the scattering matrix once the R function is found. That is, for every R^{pot} found from Eq. (17), there corresponds a potential-scattering boundary condition b_c found from Eq. (14). This is obvious when we write down the relationship between the elastic scattering S matrix element S_{cc} and the R function:

$$S_{cc} = e^{2i\phi_c} \left[1 + \frac{2iP_c R}{1 + R(b_c - S_c - iP_c)} \right]. \quad (18)$$

In this expression S_c , P_c , and ϕ_c are the well-known shift function, penetrability, and hard-sphere phase shift (all in the elastic channel c) which are dependent on the energy and on the choice of the radius parameter a_c .¹³

In summary, the scattering of a particle from a potential can be solved in one of two ways. (There are other ways, such as integral equations, not considered here.) The problem can be done exactly by matching wave functions at each energy and finding the phase shifts as a function of energy. The second approach is to use an R -matrix procedure for the partial wave of interest. The advantages of this second approach are twofold. First, it crystallizes the energy dependence of the partial wave through Eqs. (17) and (18). The other advantage is that it is the first step in an R -matrix approach to fitting the data.

B. Spectroscopic Factors in R -Matrix Theory

Potential-scattering calculations at best give only the gross features of experimental data. Examples are shown in Figs. 1 and 2.¹⁵⁻¹⁷ Here there are several resonances which cannot be fit using a simple energy-independent potential well. In order to fit such data we would like to use a simple R function of the form

$$R = R_0 + \frac{\gamma_1^2}{E_1 - E} \quad (19)$$

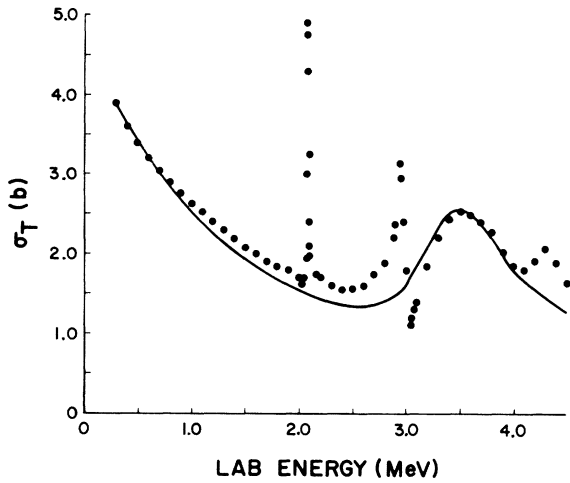


FIG. 1. Total cross section for $^{12}\text{C}(n,n)^{12}\text{C}$ from 0.5 to 4.5 MeV. The dots are experimental data taken from Refs. 15 and 16. The solid curve is a calculation using a Woods-Saxon plus spin-orbit potential. The potential parameters used were $V_0 = 62.3$ MeV, $V_{so} = 6.81$ MeV F^2 , $a = 0.408$ F, and $r_0 = 1.25$ F.

or

$$R = R_0 + \frac{\gamma_1^2}{E_1 - E} + \frac{\gamma_2^2}{E_2 - E}. \quad (20)$$

We would use Eq. (19) if there were one bump or dip of a given spin and parity. We would use Eq. (20) if there were two resonances with the same spin and parity in the energy region of interest. Equations (19) and (20) are frequently used by experimentalists. We would like to derive these equations using the procedures of many-channel

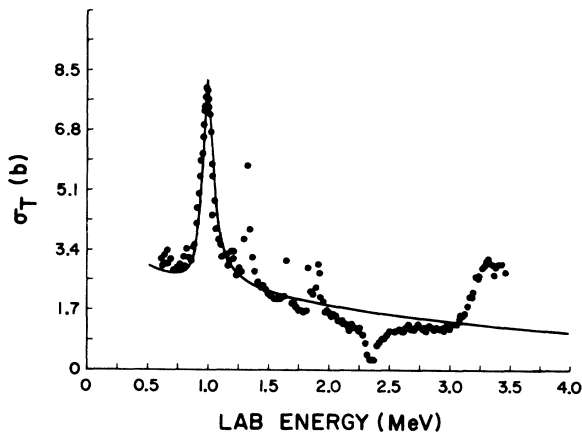


FIG. 2. Total cross section for $^{16}\text{O}(n,n)^{16}\text{O}$ from 0.5 to 3.5 MeV. The dots are experimental data taken from Ref. 17. The solid curve is a calculation using a Woods-Saxon plus spin-orbit potential. The potential parameters used were $V_0 = 54.0$ MeV, $V_{so} = 7.1$ MeV F^2 , $a = 0.61$ F, and $r_0 = 1.25$ F.

R -matrix theory and relate them to potential-scattering R functions such as Eq. (17). Once their relation to potential scattering is shown, the concept of spectroscopic factors will be discussed.

We represent the unknown full Hamiltonian by H , and the single-particle potential by H_0 . Then

$$H = H_0 + H'. \quad (21)$$

The Schrödinger equations for H and H_0 are

$$H\psi = E\psi \quad (22)$$

and

$$H_0\psi_0 = E\psi_0. \quad (23)$$

In the interior region $r_c \leq a_c$, the wave functions ψ and ψ_0 may be expanded in terms of complete sets of states χ_λ and ψ_{pc} . We then have

$$H\chi_\lambda = E_\lambda\chi_\lambda, \quad r_c \leq a_c, \quad (24)$$

$$H_0\psi_{pc} = E_{pc}\psi_{pc}, \quad r_c \leq a_c, \quad (25)$$

where χ_λ and ψ_{pc} satisfy identical boundary conditions at $r_c = a_c$.

Now, let us consider the complete set of single-particle states

$$\psi_{pc} = \phi_c u_p(r_c), \quad (26)$$

where ϕ_c is the channel wave function and $u_p(r_c)$ is the radial wave function of a single nucleon moving in a single-particle potential well. The $u_p(r_c)$ satisfy the boundary conditions

$$\frac{a_c}{u_p(a_c)} [u_p'(r_c)]_{a_c} = b_c. \quad (27)$$

The χ_λ can be expanded in terms of this complete set of single-particle states as follows:

$$\chi_\lambda = \sum_{pc} a_{\lambda; pc} \psi_{pc}. \quad (28)$$

Now, the χ_λ are antisymmetric in all nucleon coordinates, whereas ψ_{pc} is not. Thus, Eq. (28) is a fractional-parentage expansion, and the inverse does not exist.

However, consider the fully antisymmetrized ψ_{pc}^A . We could then write an equation similar to Eq. (28):

$$\chi_\lambda = \sum_{pc} \alpha_{\lambda; pc} \psi_{pc}^A. \quad (29)$$

The inverse to Eq. (29) exists:

$$\psi_{pc}^A = \sum_{\lambda} \alpha_{\lambda; pc} \chi_\lambda. \quad (30)$$

If we assume that the only important states in ψ_{pc}^A are given by ψ_{pc} then we have that

$$\psi_{pc}^A = \psi_{pc}, \quad (31)$$

$$\alpha_{\lambda; pc} = \alpha_{\lambda; pc}. \quad (32)$$

This approximation is reasonable, since the most

important target states in $\psi_{\rho c}^A$ are bound states, while the most important single-particle states are scattering states. From Eqs. (28) to (32) we can derive the conditions

$$\sum_{\lambda} a_{\lambda; \rho c} a_{\lambda; \rho' c'} = \delta_{\rho c, \rho' c'}, \quad (33)$$

$$\sum_{\rho c} a_{\lambda; \rho c} a_{\lambda'; \rho c} = \delta_{\lambda \lambda'}. \quad (34)$$

The single-particle reduced widths are given by

$$\tilde{\gamma}_{\rho c} = \left(\frac{\hbar^2}{2m_c a_c} \right)^{1/2} \int \phi_c \psi_{\rho c} dS \quad (35)$$

$$= \left(\frac{\hbar^2}{2m_c a_c} \right)^{1/2} u_p(a_c). \quad (36)$$

The reduced widths of the actual states are given by

$$\gamma_{\lambda c} = \left(\frac{\hbar^2}{2m_c a_c} \right)^{1/2} \int \phi_c \chi_{\lambda} dS \quad (37)$$

$$= \left(\frac{\hbar^2}{2m_c a_c} \right)^{1/2} \int \phi_c \sum_{\rho c} a_{\lambda; \rho c} \phi_{\rho c} u_p(a_c) dS \quad (38)$$

$$= \left(\frac{\hbar^2}{2m_c a_c} \right)^{1/2} \sum_p a_{\lambda; \rho c} u_p(a_c). \quad (39)$$

Thus,

$$\gamma_{\lambda c} = \sum_p a_{\lambda; \rho c} \tilde{\gamma}_{\rho c}. \quad (40)$$

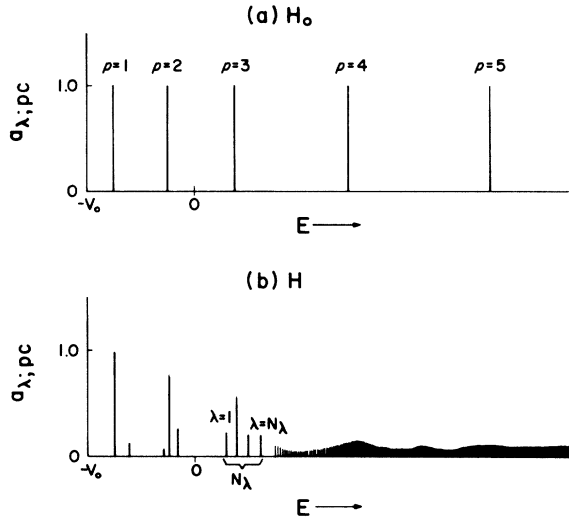


FIG. 3. A schematic diagram showing distribution of states of a given spin and parity for the single-particle Hamiltonian H_0 and the actual Hamiltonian H . The single-particle states which satisfy a specified boundary condition are shown in (a). The states corresponding to the actual Hamiltonian are shown in (b). The states $p=1$ and $p=2$ are bound states. The states $p=3, 4,$ and 5 are in the continuum. Each single-particle state p is split into several states λ . The state $p=3$ is split into states labeled from 1 to N_{λ} .

Using Eq. (33), we can derive a general relationship between the sums of the actual reduced widths and the single-particle reduced widths:

$$\sum_{\lambda} \gamma_{\lambda c}^2 = \sum_p \tilde{\gamma}_{\rho c}^2. \quad (41)$$

If we make the assumptions that, in a given energy region, only one single-particle state p contributes to the widths, and that this state p contributes only to these widths (labeled $\lambda=1$ to N_{λ}), then we get for these widths

$$\gamma_{\lambda c} = a_{\lambda; \rho c} \tilde{\gamma}_{\rho c} \quad (42)$$

and

$$\sum_{\lambda=1}^{N_{\lambda}} a_{\lambda; \rho c}^2 = 1. \quad (43)$$

The elastic scattering R matrix elements can be easily derived using standard procedures¹³ for both the complete Hamiltonian H and the single-particle Hamiltonian H_0 . The results are:

$$R_{cc}^{\text{pot}} = \sum_p \frac{\tilde{\gamma}_{\rho c}^2}{E_{\rho c} - E}, \quad (44)$$

$$R_{cc} = \sum_{\lambda} \frac{\gamma_{\lambda c}^2}{E_{\lambda} - E}, \quad (45)$$

$$R_{cc} = \sum_{\lambda} \frac{\left(\sum_{p'} a_{\lambda p'' c} \tilde{\gamma}_{p'' c} \right)^2}{E_{\lambda} - E}. \quad (46)$$

Now we want to make the same assumptions as stated above Eq. (42). We refer to Fig. 3. The states $\lambda=1$ to N_{λ} arise from the splitting of one single-particle state p . The rest of the states can be treated as an energy-independent background. We then get

$$R_{cc} = \sum_{\lambda=1}^{N_{\lambda}} \frac{a_{\lambda; \rho c}^2 \tilde{\gamma}_{\rho c}^2}{E_{\lambda} - E} + \sum_{\lambda''} \frac{\left(\sum_{p'} a_{\lambda'' p'' c} \tilde{\gamma}_{p'' c} \right)^2}{E_{\lambda''} - E}. \quad (47)$$

In this equation, the second term is the background term. This term can be approximated by assuming that

$$a_{\lambda'' p'' c} = \delta_{\lambda'' p''} \quad (48)$$

and

$$E_{\lambda''} = E_{p'' c}. \quad (49)$$

The background term then reduces to

$$\sum_{p'} \frac{\tilde{\gamma}_{p'' c}^2}{E_{p'' c} - E} = R_0. \quad (50)$$

This is exactly the same as the potential scattering R_0 computed from Eqs. (12), (15), and (16). Our Eq. (47) now becomes

TABLE I. Parameters affecting the spectroscopic factor S_λ .

Independent parameters	Determined parameters
(1) Potential-well parameters: radius, diffuseness, central well depth, spin-orbit well depth, etc.	(1) Single-particle reduced width $\tilde{\gamma}_{pc}^2$
(2) Single-particle energies E_{pc}	(2) Background term R_0
(3) R -matrix radius a_c	(3) Boundary condition b_c
	(4) Penetrabilities and shift functions

$$R_{cc} = R_0 + \sum_{\lambda=1}^{N_\lambda} \frac{a_{\lambda;pc}^2 \tilde{\gamma}_{pc}^2}{E_\lambda - E}. \quad (51)$$

This is the same as Eq. (19) or (20) if we use the connection between $\gamma_{\lambda c}^2$ and $\tilde{\gamma}_{pc}^2$ in Eq. (42):

$$\gamma_{\lambda c}^2 = a_{\lambda;pc}^2 \tilde{\gamma}_{pc}^2. \quad (52)$$

Using all of the above approximations the spectroscopic factor for the state λ can be defined as

$$S_\lambda = a_{\lambda;pc}^2 = \gamma_{\lambda c}^2 / \tilde{\gamma}_{pc}^2, \quad (53)$$

where p refers to the single-particle state in the neighborhood of λ and c is the elastic scattering channel. In order for this definition of S_λ to be meaningful, it should be relatively independent of the other parameters in the theory. The relevant parameters are given in Table I. The independent parameters are the potential-well parameters, the radius a_c , and the single-particle energies E_{pc} . The other parameters listed, such as $\tilde{\gamma}_{pc}^2$ and the boundary condition b_c are determined once the independent parameters are chosen.

Let us consider now the energy dependence of the spectroscopic factor. In order to do this we need to know how R_{cc} and R_{cc}^{pot} compare. For instance, consider the $^{12}\text{C}(n, n)^{12}\text{C}$ data and fit shown in Fig. 1. Our potential-well R matrix element is

$$R_{cc}^{\text{pot}} = R_0 + \frac{\tilde{\gamma}_{pc}^2}{E_{pc} - E}, \quad (54)$$

If we insert this into Eq. (58) and use Eq. (25) we get

$$\langle \psi_{pc} | \frac{1}{H-E} | \psi_{pc} \rangle = \frac{1}{E_{pc} - E} + \frac{1}{(E_{pc} - E)^2} \langle \psi_{pc} | H' | \psi_{pc} \rangle + \frac{1}{E_{pc} - E} \sum_{p'c'} \langle \psi_{pc} | H' | \psi_{p'c'} \rangle \frac{1}{E_{p'c'} - E} \langle \psi_{p'c'} | H' | \psi_{p''c''} \rangle \langle \psi_{p''c''} | \frac{1}{H-E} | \psi_{pc} \rangle. \quad (60)$$

This Eq. (60) cannot be solved, since H' is unknown. However, to get it into a more transparent form we assume that

$$\langle \psi_{pc} | H' | \psi_{pc} \rangle \approx 0. \quad (61)$$

This is plausible, since our single-particle potential is chosen to fit the gross features of the data. In addition we make the assumption¹³ that

$$\langle \psi_{pc} | H | \psi_{p'c'} \rangle \quad (62)$$

where E_{pc} can be varied, thus determining various values for R_0 and $\tilde{\gamma}_{pc}^2$. The R matrix element used in fitting the data is

$$R_{cc} = R_0 + \frac{S_1 \tilde{\gamma}_{pc}^2}{E_1 - E} + \frac{S_2 \tilde{\gamma}_{pc}^2}{E_2 - E}, \quad (55)$$

where S_1 , S_2 , E_1 , and E_2 are parameters used to fit the data. The boundary condition b_c is taken to be that determined by E_{pc} and a_c .

We now seek to compare Eqs. (54) and (55). We do this by expanding R_{cc} :

$$R_{cc} = R_0 + \sum_{\lambda'} \frac{S_{\lambda'} \tilde{\gamma}_{pc}^2}{E_{\lambda'} - E} \quad (56)$$

$$= R_0 + \tilde{\gamma}_{pc}^2 \sum_{\lambda'} S_{\lambda'} \langle \chi_{\lambda'} | \frac{1}{H-E} | \chi_{\lambda'} \rangle, \quad (57)$$

where λ' indicates the sum from 1 to N_λ . For the data in Fig. 1, $N_\lambda = 2$. Let us now consider only the summation in the second term in Eq. (57):

$$\sum_{\lambda'} S_{\lambda'} \langle \chi_{\lambda'} | \frac{1}{H-E} | \chi_{\lambda'} \rangle = \langle \psi_{pc} | \frac{1}{H-E} | \psi_{pc} \rangle. \quad (58)$$

Now we can expand the operator $1/(H-E)$ as follows:

$$\frac{1}{H-E} = \frac{1}{H_0-E} + \frac{1}{H_0-E} H' \frac{1}{H_0-E} + \frac{1}{H_0-E} H' \frac{1}{H_0-E} H' \frac{1}{H-E}. \quad (59)$$

have random signs so that Eq. (60) reduces to

$$\langle \psi_{pc} | \frac{1}{H-E} | \psi_{pc} \rangle = \frac{1}{E_{pc} - E} + \frac{1}{E_{pc} - E} \sum_{p'c'} \frac{|\langle \psi_{pc} | H' | \psi_{p'c'} \rangle|^2}{E_{p'c'} - E} \langle \psi_{pc} | \frac{1}{H-E} | \psi_{pc} \rangle \quad (63)$$

$$= \left(E_{pc} - E + \sum_{p'c'} \frac{|\langle \psi_{pc} | H' | \psi_{p'c'} \rangle|^2}{E_{p'c'} - E} \right)^{-1}. \quad (64)$$

Thus, our R matrix elastic scattering element can be approximated by

$$R_{cc} = R_0 + \frac{\tilde{\gamma}_{pc}^2}{E_{pc} - E + \sum_{p'c'} |\langle \psi_{pc} | H' | \psi_{p'c'} \rangle|^2 / (E_{p'c'} - E)}. \quad (65)$$

When we compare this with Eq. (55), it is not at all obvious that the spectroscopic factors S_λ are independent of the single-particle energy E_{pc} . If the S_λ are strongly dependent on the E_{pc} we have

$$S_\lambda = S_\lambda(E_{pc}). \quad (66)$$

If Eq. (66) holds, one questions the value of a quantity called the spectroscopic factor.

III. ANALYSIS OF A DOUBLE RESONANCE IN $^{12}\text{C}(n, n)^{12}\text{C}$

An interesting double resonance arises in $^{12}\text{C}(n, n)^{12}\text{C}$ data. Two broad $d_{3/2}$ resonances are found at about 2.95 and 3.50 MeV (see Fig. 1). Because they are so close together and so broad these resonances interfere with one another. Our problem is to fit this double resonance using Eq. (55), and from this fit to arrive at spectroscopic factors for these two levels. We do this by using the procedure outlined in Sec. II. That is, we find an R -matrix parametrization of the potential scattering and use these parameters to find the spectroscopic factors.

Figure 1 shows a fit to the data in which a real Woods-Saxon well with spin-orbit coupling is assumed. The well chosen is of the form

$$V_{w.s.}(r) = -V_0 \frac{1}{1 + e^{(r-R)/a}} - V_{so} 2\vec{1} \cdot \vec{s} \frac{e^{(r-R)/a}}{ar[1 + e^{(r-R)/a}]^2}, \quad (67)$$

where

$$R = r_0 A^{1/3} \quad (68)$$

and A is the mass number of the target. This potential has four parameters: a central well depth V_0 , a spin-orbit well depth V_{so} , a diffuseness a , and a radius parameter r_0 . The parameters used to generate Fig. 1 were $V_0 = 62.3$ MeV, $V_{so} = 6.81$ MeV F^2 , $a = 0.408$ F, and $r_0 = 1.25$ F. These were used by Reynolds *et al.*¹⁸ to fit the $s_{1/2}$ and $d_{3/2}$ partial waves. The phase shifts for the $s_{1/2}$ and $d_{3/2}$ waves generated by this potential agree well with those of Wills *et al.*¹⁹ However, the p -wave phase shifts are different. Several other parameter sets were tried, but this was the best set found. Since

most of the scattering in this region occurs via s and d waves, the potential gives a good over-all fit to the data.

To convert the potential-scattering calculation for the $d_{3/2}$ partial wave into an R -matrix form, we need to choose an energy E_p and an R -matrix radius a_c . Then using the wave function generated by the potential at E_p and a_c , we can compute $\tilde{\gamma}_p^2$ and b_c . Also, using the wave functions found for various other energies near E_p , we can compute $R_0(E)$ using Eq. (16). We can plot these various quantities versus E_p and a_c to see if there is a best set of values for E_p and a_c . Of course, the R function given by Eq. (10) is exact, but we would

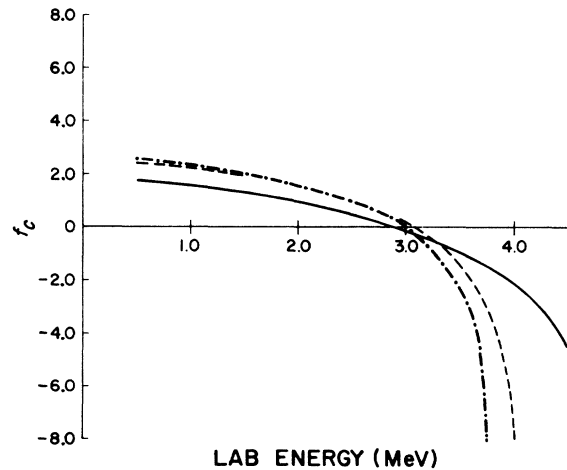


FIG. 4. Plot of $f_c(E)$ vs E for the $d_{3/2}$ partial wave in $^{12}\text{C}(n, n)^{12}\text{C}$ for various values of the R -matrix radius a_c . The solid line is for $a_c = 5.5$ F, the dashed line is for $a_c = 7.0$ F, and the dot-dashed line is for $a_c = 8.0$ F.

like to use Eq. (17). Thus, we want to choose the values of E_p and a_c which will give the least energy dependence of R_0 and $\tilde{\gamma}_p^2$ in Eq. (17) and of b_c in Eq. (18).

Figure 4 shows $f_c(E)$ vs E for various values of a_c . The boundary condition b_c is related to $f_c(E)$ through Eq. (14). Figure 5 is a plot of $\tilde{\gamma}_p^2$ vs E using various values of a_c . Figure 6 is a similar plot for R_0 . In all of these figures, the value of $a_c = 5.5$ F is as low as we can go (in steps of 0.5 F) because we must remain outside the range of the Woods-Saxon potential. If we were to make $a_c = 5.0$ F, Eq. (18) would no longer hold. The fact that a_c must be outside the range of the potential is one of the basic tenets of R -matrix theory. Some authors have ignored this basic premise in order to consider the relationship between Woods-Saxon and square-well potentials.²⁰ However, we have found that in order to reproduce almost exactly (within 0.08%) our potential-well calculation with an R function and a boundary condition, the R -matrix radius must be outside the point where the potential makes a contribution greater than about 0.1%.

Since $f_c(E)$ can go to infinity, whereas $\tilde{\gamma}_p^2$ and R_0 are always finite in our region of interest, we should consider Fig. 4 first. From Fig. 4 we see that the lower the value of a_c , the slower is the variation of $f_c(E)$ in our energy region of interest - from 0.5 to 4.5 MeV. Since $a_c = 5.5$ F is the lowest we can go and still remain outside the potential, we claim this is the best value and use it in all of our subsequent calculations. For higher values of a_c we see from Fig. 4 that $f_c(E)$ either goes to infinity or at least gets very large somewhere in our energy range. Since $f_c(E)$ behaves similar to a cotangent function, we see that to get the slowest energy variation, we must avoid values of a_c which give us $f_c(E) = \infty$ in or near our energy region of interest. Of course, at much larg-

er values of a_c we can also get away from $f_c(E) = \infty$. However, at these much larger values, the various E_p ($p \neq 1$) get much closer together so that R_0 of Eq. (13) becomes rapidly energy dependent. To keep R_0 as slowly energy dependent as possible, we must choose the lowest value of a_c which has a slowly varying $f_c(E)$ throughout the energy region of interest. It is possible that for some problems there would be no value of a_c which would give a slow enough energy dependence of $f_c(E)$, $\tilde{\gamma}_p^2$, and R_0 to reproduce the potential scattering using Eqs. (17) and (18). However, in the examples studied in this paper, such an a_c does exist.

Once we have chosen a value of a_c which gives a slowly varying $f_c(E)$, we must choose an energy E_p in order to determine b_c from Eq. (8). This is the boundary condition which is used in Eq. (18) to calculate the elastic scattering matrix element. Some uncertainty has arisen in the literature^{14, 20, 21} regarding the term "natural boundary condition." At each energy in the continuum there is a different actual nuclear wave function which is unknown. These actual nuclear wave functions have boundary conditions which oscillate with radius similar to cotangent functions. Thus, the boundary condition of the unknown true nuclear wave function varies with both energy and radius. In R -matrix theory we deal with interior and exterior wave functions. We would like our interior wave function to join smoothly with the exterior wave function at the R -matrix radius a_c . In order for this to happen at E_p we must choose Eq. (8) as our boundary condition. This makes our R -matrix wave function at E_p equal to the wave function at E_p computed from the potential well. Thus, *the natural boundary condition is given by Eq. (8)*. Our interpretation of a natural boundary condition is seen to be de-

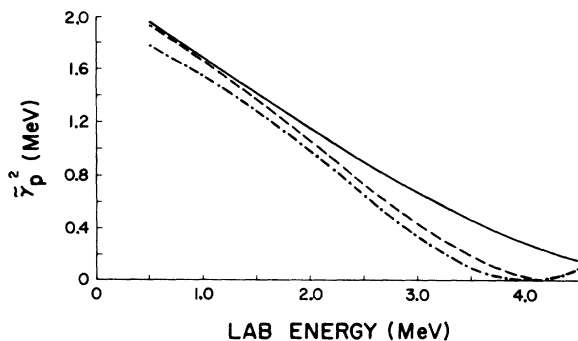


FIG. 5. Plot of $\tilde{\gamma}_p^2$ vs E for the $d_{3/2}$ partial wave in $^{12}\text{C}-(n, n)^{12}\text{C}$ for various values of the R -matrix radius a_c . The solid line is for $a_c = 5.5$ F, the dashed line is for $a_c = 7.0$ F, and the dot-dashed line is for $a_c = 8.0$ F.

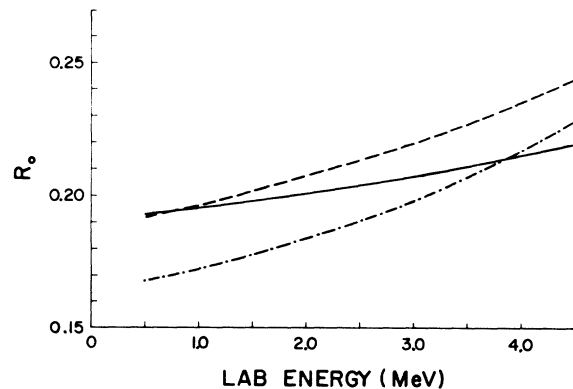


FIG. 6. Plot of R_0 vs E for the $d_{3/2}$ partial wave in $^{12}\text{C}-(n, n)^{12}\text{C}$ for various values of the R -matrix radius a_c . The solid line is for $a_c = 5.5$ F, the dashed line is for $a_c = 7.0$ F, and the dot-dashed line is for $a_c = 8.0$ F.

pendent on the parameters of the potential well and on E_p and a_c . For the well parameters we have chosen, and $E_p = 3.50$ MeV and $a_c = 5.5$ F, our natural boundary condition found from Eq. (8) was $b_c = -0.926$. Note that this is not equal to either $-l$ or zero or the shift function at E_p .

When we look at Figs. 5 and 6, we see that $a_c = 5.5$ F also gives the slowest energy dependence of $\tilde{\gamma}_p^2$ and R_0 . This, of course, is related to the fact that $f_c(E)$ is most slowly varying at this value. It also is evident from Fig. 6 and Eq. (16) that neither the value of R_0 nor the dependence of $R_0(E)$ vs E is simple. Unless an actual calculation for a particular well with a particular R -matrix radius and boundary condition is carried out, it is hard to predict either R_0 or its energy dependence. Of course, for our case, since there are no bound $d_{3/2}$ levels, we can see from Eq. (13) that R_0 will be a positive quantity, since each term in the sum is positive. For the curves shown in Fig. 6 it is necessary to choose a value of E_p to compute $R_0(E)$ from Eq. (16). Note that $E_p = E_1$ of Eq. (16). The value chosen was the peak of the resonance, or $E_p = 3.50$ MeV.

Once the best values of E_p and a_c were chosen, b_c and $\tilde{\gamma}_1^2$ were determined from Eqs. (14) and (11). Then a mean value of $R_0(E)$ was chosen as $R_0(E_p) = 0.21$. The value of R^{pot} was then computed from Eq. (17), and this was used in Eq. (18) to compute the $d_{3/2}$ portion of the total cross section from 0.5 to 4.5 MeV. In carrying out the calculation of the scattering matrix element from Eq. (18), the shift functions $S_c(E)$ and penetrabilities $P_c(E)$ were computed separately at each energy. The partial waves other than $d_{3/2}$ were computed exactly from the potential well. The calculation using the R function of Eq. (17) is exact at $E_p = 3.50$ MeV, since the energy-dependent quantities $\tilde{\gamma}_p^2$, b_c , and R_0 were computed at this energy. We found that we could reproduce the potential-scattering calculation throughout the energy range 0.5 to 4.5 MeV using Eqs. (17) and (18). A fit comparing the R -function potential-scattering calculation to the exact potential-scattering calculation is not shown, since the error is smaller than the width of the line in Fig. 1 showing the exact calculation.

In order to fit the data over the whole energy range, it was found to be important to have the correct value of R_0 . When Eq. (17) was tried with R_0 equal to zero, the R -matrix curve did not reproduce the potential calculation. The results are shown in Fig. 7. This indicates that in doing simple one-level fits to data, it is important to have the correct value of R_0 . We can see how R_0 alters the usual one-level formula if we insert Eq. (17) into Eq. (18). We can then put Eq. (18) into the form:

$$S_{cc} = e^{2i\delta_c} \left(1 + \frac{i\Gamma_p}{E_R - E - \frac{1}{2}i\Gamma_p} \right), \quad (69)$$

where

$$\delta_c = \phi_c + \tan^{-1}(R_0 P_c / D), \quad (70)$$

$$\Gamma_p = 2P_c \tilde{\gamma}_1^2 / D, \quad (71)$$

$$E_R = E_1 + \Delta, \quad (72)$$

$$\Delta = \tilde{\gamma}_1^2 [(b_c - S_c) + R_0(b_c - S_c)^2 + R_0 P_c^2] / D, \quad (73)$$

$$D = [1 + R_0(b_c - S_c)]^2 + (R_0 P_c)^2. \quad (74)$$

We see that inserting the R_0 term into the usual one-level formula drastically alters the usual fitting parameters. The hard-sphere phase shift becomes a potential-scattering phase shift, dependent on the parameters of the potential well. The values of the resonance width Γ_p and shift Δ are also changed. Note that the width Γ_p is not always decreased as some authors have claimed,²² since D can be less than unity. Also, the best boundary condition is not necessarily $b_c = S_c$, since from Eq. (73) we see that the energy shift Δ will have a nonzero value in this case. Equations (69)–(74) demonstrate the importance of having a procedure to calculate R_0 .

To fit the actual data, Eq. (20) was used. This is the usual R -matrix double-resonance formula. However, there was one important difference in our procedure. The background term R_0 was not a parameter. Instead, it was taken to be the same as in the potential-well calculation. This gave us one less parameter, and it also made data fitting much easier, since it is important to get the correct value of R_0 to fit the shape of the double res-

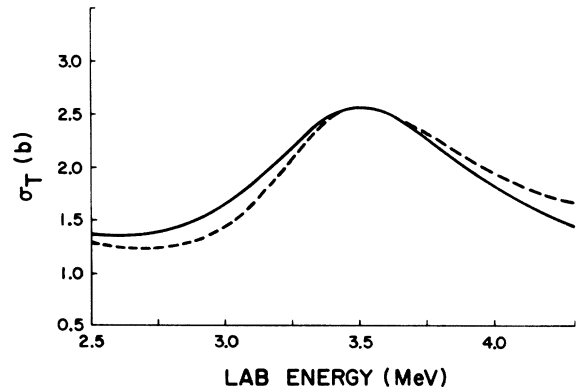


FIG. 7. An R -matrix calculation with $R_0 = 0$ compared with the potential-well calculation. The Woods-Saxon potential-well calculation is the solid curve. It is the same curve as in Fig. 1. The dashed curve uses the R -matrix formulation for the $d_{3/2}$ partial wave. All the parameters are correct except $R_0 = 0$ instead of the calculated value of 0.21.

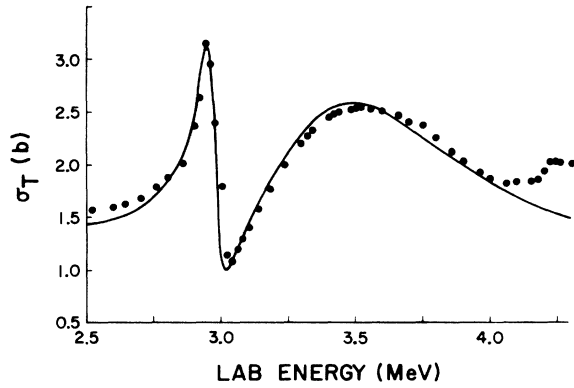


FIG. 8. A fit to the $d_{3/2}$ double resonance in $^{12}\text{C}(n, n)-^{12}\text{C}$ using the R -matrix formulation with $E_2 = 3.5$ MeV. The dots are the experimental data from Ref. 16 and the solid line is a fit using the parameters in the first line of Table II.

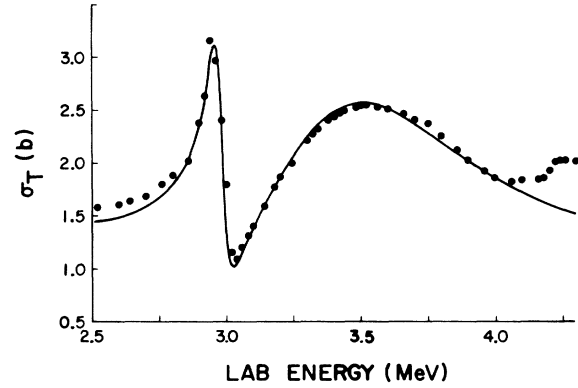


FIG. 9. A fit to the $d_{3/2}$ double resonance in $^{12}\text{C}(n, n)-^{12}\text{C}$ using the R -matrix formulation with $E_2 = 3.3$ MeV. The dots are the experimental data from Ref. 16 and the solid line is a fit using the parameters in the last line of Table II.

onance. Next, the value of E_2 was taken equal to the previous value of E_p for the single resonance calculated in Fig. 1. That is $E_2 = 3.50$ MeV. Then γ_1^2 , γ_2^2 , and E_1 were varied to get the best fit. A very good fit was obtained. It is shown in Fig. 8. The parameters used in this fit are shown in the first line of Table II. From this table we see that the spectroscopic factors for the two levels, as defined by Eq. (53), add up to 1.12 rather than unity. Thus, Eq. (43) is violated, but only by 12%. Of course, the reason for this is that the single-particle reduced width varies by about 50% over the energy range from E_1 to E_2 . Thus, it is not surprising that Eq. (43) is violated.

It is hard to know where to pick the single-particle energy in our case of a double resonance. Another possibility besides the original single-particle energy of 3.50 MeV is to pick it closer to the first resonance. When $E_p = E_2 = 3.30$ MeV was chosen, the parameters in the second line of Table II gave a good fit. This fit is shown in Fig. 9. Using this set of parameters, Eq. (43) is violated by 13%. Thus, either set gives a value of about 1.12 for the sum of the two spectroscopic factors.

What is startling about the two sets of parameters given in Table II is the tremendous difference in the value of S_1 , the spectroscopic factor of the narrow $d_{3/2}$ level. By slightly changing the energies and other parameters, we obtained two

almost equally good fits to the data, but the spectroscopic factor of the narrow level increased by more than a factor of 2. This shows that the spectroscopic factor is extremely sensitive to the energy chosen as postulated by Eq. (66). In fact, it indicates that a spectroscopic factor may be a meaningless quantity to calculate for this broad double resonance.

Before we discuss spectroscopic factors in the continuum, let us consider them in the bound-state situation. We refer to Fig. 10. In the bound-state case, energy levels have very little, if any, width associated with them. When plotted against energy, the spectroscopic factors behave like a series of δ functions, being zero at most energies, and having a nonzero value only at certain discrete energies. A theoretical calculation of energy levels and spectroscopic factors usually yields energies slightly different from the experimental values. The spectroscopic factors found in the calculation are again a series of δ functions, but with nonzero values at the calculated energies. In Fig. 10, we have indicated the experimental bound-state spectroscopic factors with solid lines, and those for the theoretical calculation with dashed lines. At the experimental energies, the theoretical calculations give spectroscopic factors of zero. What is usually done is to match the calculated and experimental spectroscopic factors, even though they

TABLE II. $^{12}\text{C}(n, n)^{12}\text{C}$ parameters for the $d_{3/2}$ double resonance.

a_c (F)	b_c	R_0	E_1 (MeV)	E_2 (MeV)	γ_1^2 (keV)	γ_2^2 (keV)	$\tilde{\gamma}_p^2$ (keV)	S_1	S_2
5.5	-0.926	0.21	2.95	3.50	68	460	470	0.14	0.98
5.5	-0.561	0.21	2.90	3.30	180	440	550	0.33	0.80

coincide with different energies.²³ The point to be made is that in the bound-state case, the spectroscopic factors are energy dependent. If another calculation is done with different parameters, a different energy dependence of spectroscopic factors will be found, since different values of energy will have nonzero spectroscopic factors. Thus, we should not be surprised that in the continuum region the spectroscopic factors are also energy dependent. This energy dependence is indicated in Fig. 10 by cross hatching the resonances in the continuum.

In the continuum we have the parameters γ_λ^2 and E_λ for each resonance. We can interpret γ_λ^2 as a measure of the spectroscopic factor at E_λ . If we change the values of E_λ as exemplified in Table II, we also expect to change γ_λ^2 . Thus, a different set of theoretical parameters yields a new set of spectroscopic factors. This is analogous to the bound-state case. The main difference seems to be that the continuum states have an energy width associated with them that is not present in the bound states. We expect the energy dependence of the spectroscopic factors to be no longer a δ function, but to spread out over their resonance width. Thus, there does not seem to be a single spectroscopic factor associated with a given continuum state.

Fortune and Vincent⁹ found that for (d, p) reactions to the continuum, the width of the resonance, rather than the spectroscopic factor, is found to be measured by the absolute magnitude of the cross section. Our Table II indicates that for the $d_{3/2}$ double resonance in the reaction $^{12}\text{C}(n, n)^{12}\text{C}$, both the reduced width γ_1^2 and the spectroscopic factor S_1 can differ by more than a factor of 2 when the energies of the resonances are changed. However, this extreme energy dependence may be due to the fact that the $d_{3/2}$ resonance at about 2.9 MeV is a broad resonance in a double-resonance situation.

IV. ANALYSIS OF A NARROW COMPOUND RESONANCE IN $^{12}\text{C}(n, n)^{12}\text{C}$

The double resonance in $^{12}\text{C}(n, n)^{12}\text{C}$ analyzed in the last section is an example of resonances very similar in width to a single-particle resonance of the same spin and parity. In this section we analyze a resonance with a very narrow width. This is the narrow $d_{5/2}$ resonance at about 2.08 MeV in the reaction $^{12}\text{C}(n, n)^{12}\text{C}$. This resonance has been analyzed by several methods.^{18, 24-28} It can be thought of as a bound state in the $^{12}\text{C}^*(2^+) + n(1d_{5/2})$ system where the neutron is in the $1d_{5/2}$ bound state.¹⁸ The 2^+ core and $\frac{5}{2}^+$ single-particle state couple to form a $\frac{5}{2}^+$ spin and parity. If this were a pure configuration, it would not be seen in ^{12}C -

$(n, n)^{12}\text{C}$. However, there is some mixing between this state and the $^{12}\text{C}(0^+) + n(1d_{5/2})$ state. Because of the mixing, the state has a small component of the $1d_{5/2}$ neutron configuration coupled to the $^{12}\text{C}(0^+)$ ground state. Thus, it can be seen in $^{12}\text{C}(n, n)^{12}\text{C}$ as a $\frac{5}{2}^+$ resonance in the continuum with a very narrow width.

If we write the wave functions of the bound $\frac{5}{2}^+$ and resonance $\frac{5}{2}^+$ states as mixtures of the two configurations mentioned above, we obtain

$$\frac{5}{2}^+(-1.10 \text{ MeV}) = a_1[(0^+) \otimes 1d_{5/2}] + a_2[(2^+) \otimes 1d_{5/2}]_{\frac{5}{2}^+}, \quad (75)$$

$$\frac{5}{2}^+(+2.09 \text{ MeV}) = a_1[(2^+) \otimes 1d_{5/2}]_{\frac{5}{2}^+} - a_2[(0^+) \otimes 1d_{5/2}], \quad (76)$$

where \otimes means vector coupling. The spectroscopic factors S_1 and S_2 are equal to a_1^2 and a_2^2 , respectively. They should sum up to unity. We also expect that S_1 will be much bigger than S_2 . By analyzing the narrow $d_{5/2}$ resonance with our methods, the value of S_2 can be determined.

The main problem in finding spectroscopic factors for such narrow resonances lies in the computation of the single-particle reduced width. We cannot use the bound state $d_{5/2}$ wave function computed at -1.10 MeV, because it falls off exponentially and S_2 computed from this wave function would approach infinity at large values of the R -matrix radius. Instead, we use the method of Schiffer²⁷ and generate a single-particle wave function at the energy of the resonance. To do this the same Woods-Saxon well was used which generated Fig. 1 except that the central potential V_0 was set equal to 47 MeV. When this was done, a broad single-particle resonance was produced in the cross section with a peak at approximately 2.08 MeV. The corresponding $d_{5/2}$ wave function and boundary con-

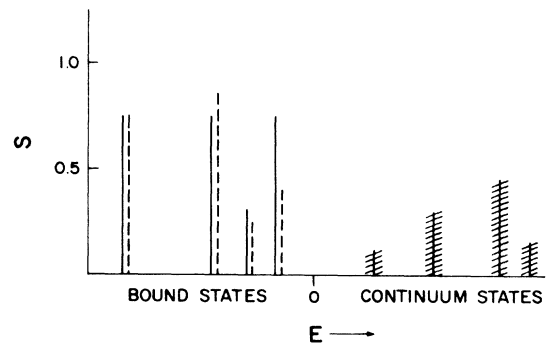


FIG. 10. Spectroscopic factors vs energy. In this schematic diagram, the solid lines indicate experimental values for bound states. The dashed lines indicate a theoretical calculation. The crossed lines in the continuum indicate resonances. These have spectroscopic factors which may or may not be well defined.

dition evaluated at an energy of 2.082 MeV was then used to compute the single-particle reduced width. This single-particle reduced width was then used in Eq. (53) to find the spectroscopic factor S_2 for the $d_{5/2}$ narrow resonance.

To fit the $d_{5/2}$ resonance we chose a value of 5.5 F for a_c . We then used the single-particle boundary condition of -1.16 in our R -matrix fit. This was necessary, since the single-particle and actual wave functions must have the same boundary conditions if we hope to compare the reduced widths. Once the parameters a_c and b_c had been chosen, we varied R_0 and γ_λ^2 to get the best fit over our energy range. All other partial waves were taken from the potential used in Fig. 1. We found that the best parameter values were $E_\lambda = 2.082$ MeV, $R_0 = 0.05$, and $\gamma_\lambda^2 = 10$ keV. Our fit is shown in Fig. 11. The single-particle reduced width was $\tilde{\gamma}_p^2 = 427$ keV, giving a spectroscopic factor of $S_2 = 0.0234$.

Next we investigated how S_2 would depend on the R -matrix radius. To do this we fit the data at various values of a_c . The various parameters used to fit the data are shown in Table III. As the R -matrix radius is increased, the data can be fitted well only over a smaller and smaller energy range, since the energy dependence of R_0 increases with increasing a_c . Note that the values of the radius were chosen where the boundary condition b_c was relatively small. This was done to decrease the energy dependence of R_0 and $\tilde{\gamma}_p^2$. It can be seen from Table III that as a_c increases, S_2 increases and then levels off at about 0.033. We believe the reason S_2 is not constant is due to the fact that at $E_\lambda = 2.082$ the single-particle wave function does not match up precisely with the actual wave function. This is evidenced by the fact

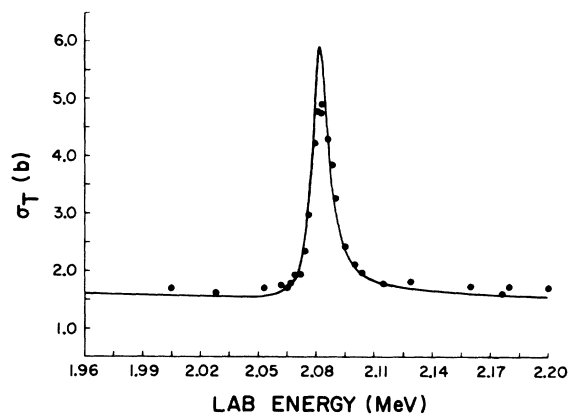


FIG. 11. The $d_{5/2}$ resonance at about 2.08 MeV in $^{12}\text{C}(n,n)^{12}\text{C}$. The dots are the experimental data from Ref. 15. The solid curve is an R -matrix calculation using the parameters indicated in the text. The spectroscopic factor for this calculation is 0.023.

that our potential well gave a cross section of about 5.0 b at 2.082 MeV, while the R -matrix fits give values of about 6.0 b at 2.082 MeV.

We conclude from Table III that the value of S_2 is 0.033 ± 0.010 . This compares favorably with the results of Bunakov, Gridnev, and Krasnov,¹² who found a value of 0.05 ± 0.03 from (d,p) data. It should be noted that they used a different single-particle neutron potential in the stripping calculations.

V. ANALYSIS OF A SINGLE-PARTICLE RESONANCE IN $^{16}\text{O}(n,n)^{16}\text{O}$

The $d_{3/2}$ resonance at about 1 MeV in $^{16}\text{O}(n,n)^{16}\text{O}$ has been the subject of several studies by (d,p) stripping methods.^{1,2,4-6} Several of these come up with the value of unity for the spectroscopic factor. Of course, the value for the spectroscopic factor will depend on the potential well chosen for the single-particle potential. We were able to find a Woods-Saxon potential which had a $d_{3/2}$ resonance at about the right energy and width to fit the resonance. The potential parameters were $V_0 = 54.0$ MeV, $V_{i0} = 7.1$ MeV F^2 , $a = 0.61$ F, and $r_0 = 1.25$ F. The solid line in Fig. 2 shows the fit to the $^{16}\text{O}(n,n)^{16}\text{O}$ data using this potential. It can be seen that the resonance at 1.0 MeV can be fit fairly well with this potential. Hence, the spectroscopic factor for this resonance is 1.0. This resonance is a trivial case for our R -matrix parametrization of spectroscopic factors. However, it is a particularly useful resonance, since the validity of various (d,p) theoretical models can be tested. However, this is by no means a "typical" resonance. It is one of the few resonances that can be fit with a simple potential-well calculation.

VI. ANALYSIS OF AN S -WAVE DIP IN $^{16}\text{O}(n,n)^{16}\text{O}$

It can be seen from Fig. 2 that a resonance dip occurs in the reaction $^{16}\text{O}(n,n)^{16}\text{O}$ at about 2.36 MeV. This dip can be thought of as due to the interference of two s -wave resonances. One of them is the bound state at -3.27 MeV in ^{17}O . This bound state then interferes with the resonance at

TABLE III. Spectroscopic factors vs R -matrix radius for the $d_{5/2}$ resonance at 2.082 MeV in $^{12}\text{C}(n,n)^{12}\text{C}$.

a (F)	E_λ (MeV)	b	R_0	$\tilde{\gamma}_p^2$ (keV)	γ_λ^2 (keV)	S_2
5.5	2.082	-1.161	0.05	427.0	10.0	0.0234
8.0	2.082	-1.248	0.20	108.7	31.4	0.0288
10.0	2.082	-2.252	0.25	38.1	1.27	0.0333
30.0	2.082	+2.394	-0.04	14.4	0.488	0.0338

2.36 MeV. The values of the level parameters including the background R_0 are such that a dip occurs.

The resonance dip was analyzed by first converting the potential parameters used in Fig. 2 into R -matrix parameters. To approximately reproduce the potential-well calculation shown in Fig. 2, the R function parameters used were $E_p = -3.268$ MeV, $\tilde{\gamma}_p^2 = 330$ keV, $R_0 = 0.19$, $a_c = 6.00$ F, and $b_c = -2.25$. Then the dip at 2.35 MeV was fit using the double-resonance R function given in Eq. (20). The parameters for the first resonance were the same as those given for the potential; the parameters for the second resonance were $E_2 = 2.36$ MeV, $\gamma_2^2 = 20$ keV. The fit is shown in Fig. 12. Once again the fact that b_c and R_0 had been computed using our potential-well wave functions enabled an easy fitting. No tedious searches for the correct background parameters were necessary.

It is not at all clear how to extract a spectroscopic factor for this dip. The ratio of γ_2^2 to $\tilde{\gamma}_p^2$ of the bound-state resonance at 6.0 F is 0.06. However, $\tilde{\gamma}_p^2$ will exponentially decrease with larger radius. In order to use the same procedure as with the $d_{5/2}$ resonance in $^{12}\text{C}(n, n)^{12}\text{C}$, we need to find a potential which gives an s -wave resonance at about 2.36 MeV. However, single-particle s -wave resonances are very broad at such energies, and due to the $1/b^2$ factor in the cross-section formula, they cannot be seen as bumps in the data. As a matter of fact, our potential well used in Fig. 2 goes through a phase shift of $\frac{1}{2}\pi$ at about 2.3 MeV. No bump is seen in the data, because the phase shift is varying much too slowly. The corresponding wave function for the s wave has a boundary condition of about +2 at 6.0 F at about 2.3 MeV. Using this boundary condition in a single-level fit with a variable R_0 and γ_λ^2 , we could not produce a dip in the cross section. Thus, the procedure used for resonance peaks does not seem to work for resonance dips. How to define a spectroscopic factor for such a dip remains an open question.

VII. DISCUSSION

Many authors^{28, 29} have recently been concerned with using a model Hamiltonian to generate a theoretical fit to nucleon scattering data. These theoretical calculations are very useful in determining how valid a particular model may be. However, they do not always yield resonances with the correct widths and energies. Since spectroscopic factors are sensitive to both resonance widths and energies, a procedure is necessary to find spectroscopic factors from experimental data. The purpose of this paper has been to give such a procedure so that spectroscopic factors could be ex-

tracted from experimental nucleon resonance data.

A recent paper by Takeuchi and Moldauer²⁸ shows how a shell-model calculation for two neutrons outside a core can be performed using R -matrix theory. It is useful to point out the difference between their approach and ours. In both approaches a single-particle potential is used as a beginning step. To this single-particle potential, they add an additional potential describing the interaction between the two valence nucleons. The Hamiltonian is then diagonalized using R -matrix theory and cross sections are computed. This is a very useful approach, and it has many nice features. It is useful to point out, however, that they did not have any experimental data with which to compare their results. Our approach has been to begin with a single-particle potential, and then to use R -matrix theory to measure how well the single-particle potential fitted experimental data. The quantitative measure of this is the spectroscopic factor. Our procedure applies to most resonances seen in neutron elastic scattering in which there are no other open channels such as inelastic scattering. Admittedly, this is a very limiting feature. However, it is not hard to extend our approach to inelastic channels or reaction channels as well. We have concentrated on fitting experimental data, since there is much interest in particle-transfer reactions in the continuum.

The case of the $^{16}\text{O}(n, n)^{16}\text{O}$ $d_{3/2}$ resonance at about 1 MeV is a straightforward and almost trivial example of a resonance with a spectroscopic factor near 1.0. Unfortunately, such resonances are the exception rather than the rule. An example of a more common type of resonance is afforded by the $d_{5/2}$ narrow resonance at about 2.08 MeV in $^{12}\text{C}(n, n)^{12}\text{C}$. This resonance is seen in elastic

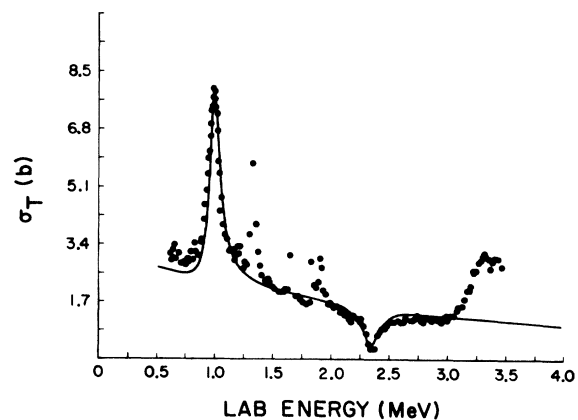


FIG. 12. The s -wave dip at about 2.36 MeV in $^{16}\text{O}(n, n)^{16}\text{O}$. The dots are the experimental data from Ref. 17. The solid curve is an R -matrix two-level fit using the parameters indicated in the text.

scattering data with a small width because there is a small amount of mixing with the $d_{5/2}$ single-particle state at -1.10 MeV. Because the mixing is small we see only a narrow resonance. The more narrow the resonance, the smaller the energy region over which we need to fit, and therefore, the less the energy dependence of the various R -matrix parameters. Thus, for such narrow resonances, the procedure for extracting spectroscopic factors is straightforward. It parallels the prevailing method used in calculating spectroscopic factors for bound states seen in stripping reactions. That is, a potential is found which gives a single-particle resonance at the energy a resonance is seen. Then, using the boundary condition for the single-particle wave function, an R -matrix fit is made to the data using γ_λ^2 and R_0 as parameters. (The resonance energy E_λ may also be slightly changed.) The spectroscopic factor is then the ratio of the reduced width used to fit the data and the single-particle reduced width. There is not a unique spectroscopic factor, since the single-particle potential parameters are not absolutely determined. Thus, one must be careful when quoting a spectroscopic factor to specify what single-particle potential-well parameters were used.

The $d_{3/2}$ double-resonance situation around 3 MeV in $^{12}\text{C}(n, n)^{12}\text{C}$ is a more difficult case for analysis. Here a single-particle resonance is

mixed quite strongly with another channel. The strong mixing yields two resonances with similar widths. Because of the strong mixing, the perturbing Hamiltonian H' is obviously not small compared to the single-particle Hamiltonian H_0 . When this case obtains, the spectroscopic factors are extremely energy dependent and hence very ambiguous.

The s -wave dip in $^{16}\text{O}(n, n)^{16}\text{O}$ proved to be very easy to fit using an R -matrix procedure of a bound-state boundary condition. However, the method of obtaining a spectroscopic factor from such a dip was not at all clear. Using a bound-state wave function, a spectroscopic factor of sorts can be obtained. However, such a spectroscopic factor will increase with increasing R -matrix radius, since the bound-state wave function decreases exponentially with increasing a_c . Thus, for the present, spectroscopic factors for resonance dips are not well defined.

ACKNOWLEDGMENTS

The authors would like to thank Dr. Donald Robson, Dr. Peter Moldauer, Dr. James Monahan, and Dr. W. Hornyak for helpful discussions concerning this work. Also special thanks go to Dr. Monahan for reading a preliminary version of the paper.

*Work supported in part by the U. S. Atomic Energy Commission and the National Science Foundation.

¹I. M. Naqib and L. L. Green, Nucl. Phys. **A112**, 76 (1968).

²V. E. Bunakov, K. A. Gridnev, and L. V. Krasnov, Phys. Letters **32B**, 587 (1970).

³H. T. Fortune, T. J. Gray, W. Trost, and N. R. Fletcher, Phys. Rev. **179**, 1033 (1969).

⁴R. Huby and J. R. Mines, Rev. Mod. Phys. **37**, 406 (1965).

⁵J. L. Alty, L. L. Green, R. Huby, G. D. Jones, J. R. Mines, and J. F. Sharpey-Schafer, Nucl. Phys. **A97**, 541 (1967).

⁶J. Bang and J. Zimányi, Nucl. Phys. **A139**, 534 (1969).

⁷V. E. Bunakov, Nucl. Phys. **A140**, 241 (1970).

⁸H. T. Fortune and C. M. Vincent, Phys. Rev. **185**, 1401 (1969).

⁹R. J. Philpott, Phys. Rev. C **2**, 1232 (1970).

¹⁰R. H. Ibarra and B. F. Bayman, Phys. Rev. C **1**, 1786 (1970).

¹¹R. Lipperheide, Phys. Letters **32B**, 555 (1970).

¹²V. E. Bunakov, K. A. Gridnev, and L. V. Krasnov, Phys. Letters **34B**, 27 (1971).

¹³A. M. Lane and R. G. Thomas, Rev. Mod. Phys. **30**, 257 (1958).

¹⁴P. J. A. Buttle, Phys. Rev. **160**, 719 (1967).

¹⁵R. O. Lane, private communication.

¹⁶*Neutron Cross Sections*, compiled by J. R. Stehn, M. D. Goldberg, B. A. Magurno, and R. Wiener-Chasman, Brookhaven National Laboratory Report No. BNL-325 (U. S. Government Printing Office, Washington, D. C., 1964), 2nd ed., Suppl. No. 2, Vol. 1.

¹⁷National Neutron Cross Section Center, Brookhaven National Laboratory.

¹⁸J. T. Reynolds, C. J. Slavik, C. R. Lubitz, and N. C. Francis, Phys. Rev. **176**, 1213 (1968).

¹⁹J. E. Wills, Jr., J. K. Blair, H. O. Cohn, and H. B. Willard, Phys. Rev. **109**, 891 (1958).

²⁰E. Vogt, Rev. Mod. Phys. **34**, 723 (1962).

²¹M. Danos and W. Greiner, Phys. Rev. **146**, 708 (1966).

²²C. B. Dover, C. Mahaux, and H. A. Weidenmüller, Nucl. Phys. **A139**, 593 (1969).

²³N. Auerbach, Phys. Rev. **163**, 1203 (1967).

²⁴J. E. Purcell, Phys. Rev. **185**, 1279 (1969).

²⁵T. Lovas, Nucl. Phys. **81**, 353 (1966).

²⁶T. T. Leung and R. D. Koshel, Bull. Am. Phys. Soc. **16**, 78 (1971).

²⁷J. P. Schiffer, Nucl. Phys. **46**, 246 (1963).

²⁸K. Takeuchi and P. A. Moldauer, Phys. Rev. C **2**, 925 (1970).

²⁹C. Mahaux and H. A. Weidenmüller, *Shell-Model Approach to Nuclear Reactions* (John Wiley & Sons, New York, 1969), and references cited therein.